Application of the quasiGaussian entropy theory to the calculation of thermodynamic properties of water and methane in the liquid and gas phase

M. E. F. Apol, A. Amadei, and H. J. C. Berendsen

Citation: The Journal of Chemical Physics **104**, 6665 (1996); doi: 10.1063/1.471385
View online: http://dx.doi.org/10.1063/1.471385
View Table of Contents: http://scitation.aip.org/content/aip/journal/jcp/104/17?ver=pdfcov
Published by the AIP Publishing

Application of the quasi-Gaussian entropy theory to the calculation of thermodynamic properties of water and methane in the liquid and gas phase

M. E. F. Apol, A. Amadei, and H. J. C. Berendsen
Groningen Biomolecular Sciences and Biotechnology Institute (GBB), Department of Biophysical Chemistry, University of Groningen, Nijenborgh 4, 9747 AG Groningen, The Netherlands

(Received 27 December 1995; accepted 24 January 1995)

In this article we investigate the applicability of the statistical Gamma state as following from the quasi-Gaussian entropy theory, where all thermodynamic properties at every temperature are obtained from the knowledge of the potential energy distribution at one temperature. We compared for a typically polar system (water) and an apolar one (methane) the experimental heat capacity and entropy data with the predictions of the theory at various densities, ranging from the almost ideal gas to typical liquids. Interestingly, the behavior of water and methane is quite similar. Low-density gases and fluid-liquid systems can be described as weakly perturbed Gamma states. For intermediate densities a more complex statistical state arises. In order to describe more accurately the fluid-liquid regime, we propose in this paper a confined Gamma state, based on the division of phase-space into two different regions: one of them described by an exact Gamma state and another very unstable one. We conclude that typical fluid-liquids can be described very well by this new Gamma state approximation. We also try to give a physical interpretation of the two parts of phase space that arise from the model. The high accuracy of the theory over a large temperature range makes the approach very suitable for the prediction of thermodynamical properties at, for example, supercritical conditions. [S0021-9606(96)00317-X]

I. INTRODUCTION

The use of (empirical) fitting functions of thermodynamic properties or equations of state is often not very satisfactory because of the lack of a full physical consistency and the need of a large dataset to extract the parameters. The possibility to obtain predictions of thermodynamic properties or an equation of state, based on a coherent physical theory which would require only a limited set of initial data (preferably measured at moderate conditions), could be of great importance.

In this paper we apply a recently introduced physical theory, the quasi-Gaussian entropy theory, to predict the temperature dependence of various thermodynamic properties at a given density from the knowledge of the internal energy, entropy, heat capacity, and its temperature derivative at one (moderate) initial temperature. In a recent article[1] we described a way of calculating excess thermodynamic properties, like excess free energy, entropy, potential energy, and heat capacity, based on knowledge of the shape of the potential energy distribution function. As the excess free energy is uniquely related to the moment generating function (Laplace transform) of the potential energy distribution, it follows that all thermodynamic properties can be derived from the knowledge of this distribution. Each different type of distribution therefore defines a different ''statistical state'' of the system, with its own specific equilibrium physics. A schematic diagram of the theory is given in Fig. 1.

We used a generalization of the Pearson system of frequency curves[1,2] to generate a set of different (potential energy) distribution functions, with increasing complexity. The simplest solutions are the Gaussian and Gamma distribution. We derived expressions for the thermodynamic properties in terms of the parameters of these distributions, which in turn can be related to (temperature derivatives of) the heat capacity C_V. Using the thermodynamic relation $\partial S/\partial T = C_V/T$ we were also able to obtain the temperature behavior of these thermodynamic properties. Knowledge of C_V (Gaussian state) or C_V and $\partial C_V/\partial T$ (Gamma state) at one temperature is sufficient to predict the temperature behavior of the heat capacity and the entropy. Combined with the knowledge of the initial internal energy, also the internal energy and the free energy can be calculated as a function of temperature.

In the same article we also tested the Gamma state solution on liquid water and methanol, finding that both liquids could be considered as weakly perturbed Gamma states, still well described by a simple Gamma state approximation (effective Gamma state). Another interesting feature of these liquids was the fact that the intrinsic entropy function α, i.e., the ratio between excess entropy and heat capacity, is very temperature insensitive over a large temperature interval.

In this paper we will investigate the effect of the density on the thermodynamic properties of water and methane (the entropy, the heat capacity, and the intrinsic entropy function) and the quality of the Gamma state description. For low density gas conditions a left-skewed Gamma distribution is introduced, defining the special negative Gamma state (Γ_-). For fluid-liquid conditions a confined Gamma approximation is proposed, based on the division of the phase-space into two different regions, one of which is described by an exact Gamma state and the other is completely unstable. Such a model provides a very accurate description of the fluid-liquid regime, a weakly perturbed Gamma state condition. Interest-

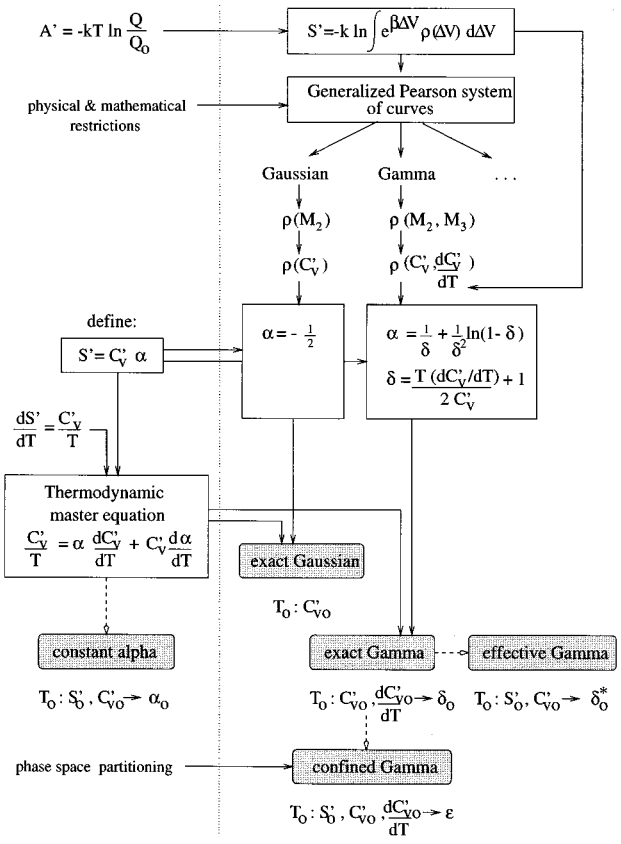

FIG. 1. A schematic diagram of the quasi-Gaussian entropy theory. Left of the dotted line are the input equations, approximations are denoted by dashed arrows. The input data at T_0 to calculate $S'(T)$ and $C'_V(T)$ are given below the different solutions. For all solutions with the knowledge of U'_0 also $A'(T)$ and $U'(T)$ can be obtained.

ingly, the Gamma region, where fluid-liquid systems are completely confined, could be connected with the restrictions in molecular organization, arising at increasing density.

The paper is organized as follows. The first two theory sections are a summary of the quasi-Gaussian entropy theory described in detail previously,[1] while in Sec. II C we introduce the special Γ_- state and in Sec. II D we describe the new confined Gamma approximation based on the double state model (in Appendix B we give a general description of this model). In the results part we investigate for both water and methane the effect of the density (ranging from the almost ideal gas to a typical liquid) and the polarity on the applicability of the Gamma state descriptions.

II. THEORY

A. Introduction

For clarity a schematic diagram is presented in Fig. 1, summarizing the theory and the various approximations, described previously[1] and in this article. The macroscopic molecular systems under consideration are (as usual) assumed to be in the quasiclassical limit. This means that apart from quantum bond and angle vibrations, all other interactions are described classically. In that case the excess (or *ideal reduced*) Helmholtz free energy of a system, i.e., the free energy with respect to a system with the same temperature and density and the same bond and angle constraints (if present) but with no intermolecular and intramolecular interactions and no vibrations[3] is given by[1]

$$A' = A - A_0 = kT \ln\langle e^{\beta \mathscr{V}} \rangle \tag{1}$$

$$= U' + kT \ln\langle e^{\beta y} \rangle. \tag{2}$$

Here A and A_0 are the full free energies of the actual system and the reference state, $\mathscr{V}$ is the total potential energy of the system (including possible quantum vibrational energies), $U' = \langle \mathscr{V} \rangle$ is the (ideal reduced) internal energy, $y = \mathscr{V} - \langle \mathscr{V} \rangle$ is the potential energy fluctuation and $\beta = 1/kT$. Angular brackets denote a canonical ensemble average and the prime stands for ''ideal reduced.''

Equation (2) can be rewritten in terms of the potential energy distribution function $\rho(y)$ as

$$A' = U' + kT \ln \int e^{\beta y} \rho(y) dy, \tag{3}$$

where $\rho(y)dy$ is the probability of finding a potential energy fluctuation between y and $y+dy$. Thus if we know the energy distribution, all equilibrium physics follows from that, since

$$S' = -\left(\frac{\partial A'}{\partial T}\right)_V = \frac{U' - A'}{T} = -k \ln \int e^{\beta y} \rho(y) dy, \tag{4}$$

$$C'_V = T\left(\frac{\partial S'}{\partial T}\right)_V, \tag{5}$$

etc.

Equation (1) indicates that the (ideal reduced) free energy is proportional to the logarithm of the moment generating function[4] (or Laplace transform) of the total potential energy distribution function, whereas Eq. (4) shows that the ideal reduced entropy S' is proportional to the logarithm of the moment generating function of the distribution of the potential energy fluctuations.

If the macroscopic system can be thought to be built up from a large collection of identical, independent subsystems (elementary systems) which are still thermodynamically defined, we can apply the central limit theorem to show that $\rho(y)$ must be uninormal and close to a Gaussian distribution. Using a generalized Pearson system of frequency curves[1,2] we can generate distributions with increasing complexity which satisfy the mathematical and physical restrictions that we can impose.[1] The solutions of this Pearson system can be used to classify the physical systems into different ''statistical states,'' since the shape of ρ uniquely determines the kind of physics. The two simplest possible solutions (see also Fig. 1) are the Gaussian distribution,

$$\rho(y) = (1/\sqrt{2\pi b_0}) \exp\left(-\frac{y^2}{2b_0}\right) \tag{6}$$

and the Gamma distribution,

$$\rho(y)=\frac{b_1(1/b_1^2)^{b_0/b_1^2}}{\Gamma(b_0/b_1^2)}(b_0+b_1y)^{b_0/b_1^2-1}\exp[-(b_0+b_1y)/b_1^2] \tag{7}$$

with $\Gamma(\cdot)$ the Gamma function[5] and where the parameters b_0 and b_1 are related to the central moments $M_n=\langle y^n\rangle$ of the energy distribution in the following way:

$$b_0=M_2, \tag{8}$$

$$b_1=\frac{M_3}{2M_2}. \tag{9}$$

Using standard statistical mechanical relations,[6,7] we can link these moments to (temperature derivatives of) the ideal reduced isochoric heat capacity C_V', obtaining

$$b_0=kT^2C_V', \tag{10}$$

$$b_1=kT+\frac{kT^2(\partial C_V'/\partial T)_V}{2C_V'}. \tag{11}$$

Hence with the knowledge of U', C_V', and $\partial C_V'/\partial T$ all thermodynamical properties are defined in the ''Gamma state.'' For the ''Gaussian state'' just U' and C_V' are sufficient. Further solutions of the Pearson system will not be considered here, partly because of their increased mathematical complexity and partly because already the Gamma state is sufficient to approximate in many different cases the actual statistical state of the system.

B. Intrinsic entropy function and thermodynamic master equation

We also introduced the concept of the *intrinsic entropy function*[1] α, a dimensionless and intensive quantity, defined as

$$\alpha=\frac{S'}{C_V'}. \tag{12}$$

Since the ideal reduced entropy is always negative and C_V' positive, this means that $\alpha<0$. The meaning of α becomes more evident by rewriting Eq. (12) as

$$\alpha=\frac{S'}{C_V'}=\left(\frac{(\partial S'/\partial T)_V}{S'/T}\right)^{-1}=-\left(\frac{(\partial S'/\partial\beta)_V}{S'/\beta}\right)^{-1}. \tag{13}$$

Since $S'=0$ when $\beta=0$, α is thus the ratio between the average slope of S' vs β and the instantaneous slope $\partial S'/\partial\beta$. If for instance $|\alpha|>1$ the instantaneous slope is smaller than the average slope in absolute values, meaning that the system has a large ''resistance'' against increasing the order by lowering the temperature.

In Appendix A we derive the high temperature limit of α:

$$\lim_{T\to\infty}\alpha(T)=-\tfrac{1}{2}. \tag{14}$$

The value $\alpha=-\frac{1}{2}$ corresponds to the Gaussian state condition, implying that at infinite temperature for every system the thermodynamics is indistinguishable from that of a Gaussian state. For example we find that in this high temperature limit $S'(\beta)\propto\beta^2$.

Since $S'=C_V'\alpha$ we can obtain an analytical expression for α using Eq. (4) if the distribution is known. We can closely link α and C_V' via their temperature derivatives. Using the fact that $(\partial S'/\partial T)_V=C_V'/T$ we obtain the *thermodynamic master equation*[1]

$$\frac{C_V'}{T}=\alpha\left(\frac{\partial C_V'}{\partial T}\right)_V+C_V'\left(\frac{\partial\alpha}{\partial T}\right)_V. \tag{15}$$

If at a certain temperature we know the exact statistical state of the system (i.e., we know the analytical shape of the energy distribution defined by a set of parameters in terms of energy moments, which can be linked to temperature derivatives of C_V'), we can calculate the integral in Eq. (4) to obtain an analytical expression of S' in terms of T, C_V', $\partial C_V'/\partial T$, etc. and, hence, of $S'/C_V'=\alpha(T,C_V',\partial C_V'/\partial T,\ldots)$. Then Eq. (15) forms a completely defined differential equation in C_V' and T (see also Fig. 1), the solution of which yields $C_V'(T)$ and all its temperature derivatives in T, given the values of $C_{V0}',\partial C_{V0}'/\partial T,\ldots$ at one temperature T_0 as boundary conditions. From that we can obtain $\alpha(T)$, the entropy via $S'(T)=C_V'(T)\alpha(T)$, the potential energy via $U'(T)=U_0'+\int_{T_0}^{T}C_V'(T)dT$ and finally $A'(T)=U'(T)-TS'(T)$. In the next section we will investigate in detail the expressions of the Gamma state.

C. Properties of the Gamma state

The free energy of the Gamma state can be readily calculated, evaluating the integral in Eq. (3) using Eqs. (7), (10), and (11) to obtain[1]

$$A'=U'-TC_V'\left[\frac{1}{\delta}+\left(\frac{1}{\delta}\right)^2\ln(1-\delta)\right], \tag{16}$$

where

$$\delta=\frac{b_1}{kT}=\frac{T(\partial C_V'/\partial T)}{2C_V'}+1 \tag{17}$$

and, hence,

$$\alpha(\delta)=\frac{S'}{C_V'}=\frac{1}{\delta}+\left(\frac{1}{\delta}\right)^2\ln(1-\delta). \tag{18}$$

The quantity δ is a measure for the asymmetry of the energy distribution. For physical reasons, since the free energy must be a finite value and, hence, the integral in Eq. (3) must converge, we find that

$$\delta<1. \tag{19}$$

Furthermore, the sign of δ indicates if we are dealing with a left-skewed Gamma distribution ($\delta<0$) defining a negative Gamma state (Γ_-) or a right-skewed Gamma distribution ($\delta>0$) defining a positive Gamma state (Γ_+). The value $\delta=0$ corresponds to a perfectly symmetrical distribution, i.e., a Gaussian.

It is important to note that in a negative Gamma state the energy distribution is defined from $-\infty$ to a finite upper energy limit, as follows from Eq. (7) in the case that $kT\delta = b_1 < 0$. For a positive Gamma state, on the contrary, the distribution has a finite lower energy limit, and is defined up to $+\infty$. This implies that only the positive Gamma state can be considered as a real physical statistical state, fulfilling all the physical and mathematical restrictions,[1] while the negative Gamma state must be regarded as a numerical approximation of a more complex statistical state.

To solve the thermodynamic master equation, we first have to solve the differential equation written in terms of $\delta(T)$ and from that obtain the solution of $C_V'(T)$. We finally find[1]

$$\delta(T) = \frac{T_0\delta_0}{T(1-\delta_0)+T_0\delta_0}, \tag{20}$$

$$C_V'(T) = C_{V0}'\left(\frac{T_0}{T(1-\delta_0)+T_0\delta_0}\right)^2 = C_{V0}'\left(\frac{\delta(T)}{\delta_0}\right)^2, \tag{21}$$

$$S'(T) = C_V'(T)\left[\frac{1}{\delta(T)} + \left(\frac{1}{\delta(T)}\right)^2 \ln[1-\delta(T)]\right], \tag{22}$$

$$U'(T) = U_0' + T_0 C_{V0}' \frac{(T-T_0)}{T(1-\delta_0)+T_0\delta_0}$$

$$= U_0' + (T-T_0)C_{V0}'\left(\frac{\delta(T)}{\delta_0}\right), \tag{23}$$

$$A'(T) = U_0' - \frac{T_0 C_{V0}'}{\delta_0} - \frac{TC_{V0}'}{\delta_0^2}\ln\left(\frac{T(1-\delta_0)}{T(1-\delta_0)+T_0\delta_0}\right)$$

$$= U_0' - \frac{T_0 C_{V0}'}{\delta_0} - \frac{TC_{V0}'}{\delta_0^2}\ln\left(\frac{T(1-\delta_0)}{T_0}\,\frac{\delta(T)}{\delta_0}\right), \tag{24}$$

where C_{V0}', U_0', and δ_0 are the values of C_V', U', and δ at the arbitrary reference temperature T_0, and δ_0 is calculated using Eq. (17).

These expressions have a finite limit for $T\to\infty$ for both the positive and negative Gamma state. By expanding the logarithm we obtain

$$\lim_{T\to\infty}\delta(T) = \lim_{T\to\infty}C_V'(T) = \lim_{T\to\infty}S'(T) = 0, \tag{25}$$

$$\lim_{T\to\infty}A'(T) = \lim_{T\to\infty}U'(T) = U_0' + \frac{T_0 C_{V0}'}{1-\delta_0}. \tag{26}$$

The low temperature limit though is different for both distributions. For a positive Gamma state (Γ_+) we find the following limits for $T\to 0$:

$$\lim_{T\to 0}\delta(T) = 1, \tag{27}$$

$$\lim_{T\to 0}C_V'(T) = \frac{C_{V0}'}{\delta_0^2}, \tag{28}$$

$$\lim_{T\to 0}S'(T) = -\infty, \tag{29}$$

$$\lim_{T\to 0}A'(T) = \lim_{T\to 0}U'(T) = U_0' - \frac{T_0 C_{V0}'}{\delta_0}. \tag{30}$$

For a negative Gamma state (Γ_-), however, the solution of the master equation in temperature encounters a singularity at a temperature $T_*>0$. The singularity occurs when the denominator in Eq. (20) is zero, i.e.,

$$T_* = -T_0\delta_0/(1-\delta_0). \tag{31}$$

The $T\to T_*$ limits in this case are

$$\lim_{T\to T_*}\delta(T) = \lim_{T\to T_*}S'(T) = \lim_{T\to T_*}U'(T)$$

$$= \lim_{T\to T_*}A'(T) = -\infty, \tag{32}$$

$$\lim_{T\to T_*}C_V'(T) = \infty. \tag{33}$$

Note that $\partial C_V'/\partial T > 0$ for all T in the case of a Γ_+ distribution, and for all $T>T_*$ in the case of a Γ_- distribution.[8]

Another distinction between the positive and negative Gamma state is the domain of α, the intrinsic entropy function. One can prove that

$$-\tfrac{1}{2} < \alpha < 0 \quad \text{for} \quad \delta < 0 (= \Gamma_-),$$

$$\alpha < -\tfrac{1}{2} \quad \text{for} \quad 0 < \delta < 1 (= \Gamma_+). \tag{34}$$

Although the positive Gamma state is compatible with all the mathematical and physical restrictions we formulated,[1] it cannot be an exact physical solution at every temperature. The reason is the behavior of C_V' as $T\to 0$: from a thermodynamical point of view, both the heat capacity of the system and that of the reference state must tend to zero as $T\to 0$, because of Nernst heat theorem[9] ($S=0$ at $T=0$). Therefore C_V' must tend to zero as $T\to 0$ as well. This is obviously not the case for both Gamma states. Therefore even the positive Gamma state cannot be considered a physical statistical state for systems in the limit $T\to 0$. This restriction in the applicability of the positive Gamma state is connected with the emerging quantum character of the system in the low temperature limit. However for systems in the liquid or gas phase, the $T\to 0$ limit is never encountered, since at constant volume there is a phase transition from a liquid or gas with homogeneous density to a liquid or solid in equilibrium with a gas.

There is another important difference between the negative and positive Gamma state. The energy difference between the average, $\langle\mathscr{V}\rangle$, and the lower (or upper) limit of the distribution $\mathscr{V}_0$, given by[1] $y_0 = \mathscr{V}_0 - \langle\mathscr{V}\rangle = -b_0/b_1 = -TC_V'/\delta$, tends to $-T_0C_{V0}'/(\delta_0(1-\delta_0))$ as $T\to\infty$. For a negative Gamma state we find $\lim_{T\to\infty}y_0>0$ while a positive Gamma state yields $\lim_{T\to\infty}y_0<0$. If we look at the temperature derivative of this difference, we find $\partial y_0/\partial T = -T_0^2C_{V0}'/[T(1-\delta_0)+T_0\delta_0]^2 < 0$ for both states. Thus the absolute difference $|y_0|$ increases to a maximum for a positive Gamma state, whereas $|y_0|$ decreases to a minimum for a negative Gamma state. This means that in the high temperature limit the corresponding left-skewed Gamma distribution is more or less ''squeezed.'' This implies that the latter can

only be a reasonable approximation up to a certain temperature. As soon as the average energy is approaching the upper energy limit too much, the approximation of the real physical statistical state by a negative Gamma state will break down.

Therefore, the negative Gamma state must be regarded always as an approximation of the real statistical state of the system, while the positive Gamma state, from a certain temperature on, might be considered the real statistical state of the system. An exact right-skewed Gamma distribution is obtained[1] for the potential energy distribution of a collection of classical harmonic oscillators coupled to a temperature bath, which is a good model for a solid in the classical limit,[10] i.e., $T \gg \hbar\omega_0/k$.

D. Approximated solutions of the thermodynamic master equation

In this section we will describe different approximated solutions of the thermodynamic master equation, Eq. (15), two of which are based on the assumption that the real statistical state is (very) close to a Gamma state, a perturbed Gamma state condition (see also Fig. 1).

The first approximation is the *effective Gamma state*.[1] It provides the ''closest'' Gamma state solution to the real statistical state around the reference temperature T_0. The entropy at the reference temperature is used to calculate the effective δ_0^* via Eq. (18), i.e., solving

$$S_0'/C_{V0}' = \alpha_0 = 1/\delta_0^* + (1/\delta_0^*)^2 \ln(1-\delta_0^*).$$

With this effective δ_0^* Eqs. (20)–(24) can be used. It must be noted that in the case of an exact Gamma state the values of δ_0 obtained from Eqs. (17) and (18) must be equal. In the case of a perturbed Gamma state on the other hand both equations will provide somewhat different values and Eq. (18) is used to calculate δ_0^* as in this way the approximated Gamma solution will reproduce the entropy and, hence, the free energy of the system very efficiently. This effective Gamma state proved to be a general good approximation for liquid water and methanol.[1]

The second approximated solution of the thermodynamic master equation is the *constant alpha approximation*.[1] Here it is assumed that the last term in Eq. (15) is negligible with respect to the other terms. This means that $\partial\alpha/\partial T \sim 0$ and, hence, $\alpha(T) \cong \alpha_0$. This simplifies the master equation considerably, and we obtain

$$C_V'(T) = C_{V0}' \left(\frac{T}{T_0}\right)^{\lambda_0}, \tag{35}$$

$$U'(T) = U_0' + \frac{C_V'(T)T}{\lambda_0+1} - \frac{C_{V0}'T_0}{\lambda_0+1}, \tag{36}$$

$$A'(T) = U_0' - \frac{C_{V0}'}{\lambda_0+1}\left[\alpha_0 T\left(\frac{T}{T_0}\right)^{\lambda_0} + T_0\right], \tag{37}$$

where

$$\lambda_0 = \frac{1}{\alpha_0}. \tag{38}$$

This approximation turned out to be an excellent description for liquid water and methanol over a large temperature range.[1] However, it can not be a global solution, since in the limit of infinite temperature α must tend to $-\frac{1}{2}$, see Eq. (14). Note that this approximation is, in principle, independent from the choice of the potential energy distribution function following from the generalized Pearson system.

In this paper we introduce a new approximation for perturbed Gamma state conditions, the *confined Gamma state*, based on a double state model. In Appendix B we derive the general equations for the ideal reduced free energy, entropy, energy, and heat capacity, based on the division of phase space into two subspaces. By assuming that one of these subspaces is very unstable (i.e., the free energy of that part of phase space is much higher than the free energy of the other part, meaning that the system is completely confined within the stable part), and assuming that the stable subspace is exactly described by a Gamma state (Γ) we obtain

$$C_V'(T) = C_V^{\Gamma'}(T), \tag{39}$$

$$S'(T) = S^{\Gamma'}(T) + k \ln \epsilon, \tag{40}$$

$$U'(T) = U^{\Gamma'}(T), \tag{41}$$

$$A'(T) = A^{\Gamma'}(T) - kT \ln \epsilon, \tag{42}$$

$$\rho(\mathscr{X}) = \rho^{\Gamma}(\mathscr{X}), \tag{43}$$

where the ''Γ'' superscript refers to the pure Γ equations [Eqs. (21)–(24) and (7)] and ϵ is the volume fraction of phase space corresponding to the Γ region. Note that only S' and A' are corrected for the presence of the other unstable part of phase space.

As already mentioned this approximation is only applicable in the case of a perturbed Gamma state. Such an approach can be considered than as a more sophisticated Gamma state approximation than the effective Gamma state. However, it must be noted that in the infinite temperature limit this new approximation cannot be valid, because in this limit the difference in stability of the two states in reality will tend to zero. In this approach though S' tends to a constant different from zero. The effective Gamma state approximation on the contrary still provides a proper behavior in the infinite temperature limit.

E. Application to small molecules

From a practical point of view, the measurable quantities are the *reduced* properties instead of the ideal reduced properties, i.e., with respect to a reference system with no intermolecular interaction (physical ideal gas). The reduced free energy A^r can be written in general as[1]

$$A^r = A' - A_0' = kT \ln\langle e^{\beta\nu}\rangle - kT \ln\langle e^{\beta\nu^0}\rangle_0, \tag{44}$$

where ν^0 includes only semiclassical intramolecular interactions and quantum vibrations. For small molecules like water and methane, however, the intramolecular interactions are not present or can be neglected, and therefore ν^0 only contains the quantum vibrational energy E^0.

For small molecules with a large seperation between the vibrational energy levels for a large range of temperature Eq. (44) becomes[1]

$$A^r = kT \ln\langle e^{\beta\nu}\rangle - E_0^0 \tag{45}$$

with E_0^0 the total vibrational groundstate energy of the ideal gas, which is independent from the temperature. In this case therefore $S^r = S'$, $C_V^r = C_V'$, and $U^r = U' - E_0^0$.

For small molecules where excited vibrational states are accessible, assuming that in the real system the vibrational energy is independent from the semiclassical coordinates, Eq. (44) reduces to

$$A^r = kT \ln\langle e^{\beta\Phi}\rangle \tag{46}$$

with Φ the intermolecular interaction energy, as in this case $\langle e^{\beta\nu}\rangle = \langle e^{\beta\Phi}\rangle\langle e^{\beta E}\rangle$ and $\langle e^{\beta E}\rangle = \langle e^{\beta E^0}\rangle_0$ where E is the quantum vibrational energy of the real system. We can thus use the quasi-Gaussian entropy theory to express $\langle e^{\beta\Phi}\rangle$ in terms of $\langle\Phi\rangle = U^r$ and central moments of Φ, and to express the thermodynamic master equation in reduced properties. Hence in this case we can apply the equations of the previous section directly to the reduced properties.

III. RESULTS

Here we present a survey for water and methane at various densities, ranging from the almost ideal gas to typical liquids. We focus mainly on the reduced entropy and isochoric heat capacity, since they are the most sensitive quantities and $U^r = \int C_V^r dT$ and $A^r = -\int S^r dT$ are determined by these quantities up to a constant. Therefore, a consistent prediction of both S^r and C_V^r means that also ΔU^r and ΔA^r will be predicted with comparable accuracy. Moreover, we will use the intrinsic entropy function α to judge the quality of the various predictions (effective Gamma, confined Gamma, and constant alpha approximation).

In the previous article[1] we showed that for water we can calculate the reduced properties via Eq. (45), since the first vibrational energy gap is much larger than kT, at least up to 1000 K. For methane on the contrary, because of anharmonicity,[11,12] already at moderate temperature excited states are accessible. In this case we assume the vibrations to be independent from the environment and therefore we can calculate the reduced properties via Eq. (46).

In all cases we calculated the excess quantities using tabulated values of the entropy and, if available, the isochoric heat capacity. If not available, the heat capacity was calculated from the entropy via $C_V^r = T(\partial S^r/\partial T)_V$. As reference state we chose for both systems a density (or pressure) close enough to the ideal gas condition for the whole temperature range we investigated. For water we used for that purpose data measured at 0.01 bar, for methane we used a density of 0.001 mol/dm^3. The molar reduced entropy was calculated as

$$S^r(T,\rho) = S(T,\rho) - S_0(T,\rho_0) + R \ln\frac{\rho}{\rho_0}, \tag{47}$$

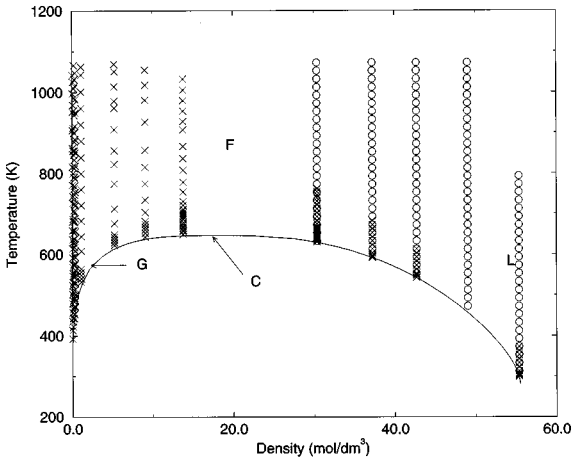

FIG. 2. The covered part of the ρ,T diagram of water, based on data from Schmidt (Ref. 11) (×) and Burnham *et al.* (Ref. 12) (○). C denotes the critical point, and G, L, and F denote gas, liquid, and fluid phase (conditions above the critical temperature), respectively.

where the last term on the right-hand side is the correction of the ideal gas entropy due to the change of density.

The experimental data for water were taken from Schmidt.[13] The covered part of the ρ,T phase diagram is represented in Fig. 2. The data on the liquid side are severely limited at high temperature because of the pressure, as the density has to be fixed; experimental data are given by Schmidt up to 1000 bar, and this especially affects the liquid region (see, for example, Obert and Gaggioli[9] for the pVT surface of water). We therefore also included high-pressure data (100–10 000 bar) from Burnham *et al.*[14] Previously[1] we presented data for the reduced free energy at 55.32 mol/dm^3 (the largest density in Fig. 2) over a large temperature range, using liquid-vapor equilibrium data. However we had to make several corrections, which were difficult to evaluate within 0.5 kJ/mol at temperatures above ~500 K, say. Hence, the numerical calculation of S^r and C_V^r from these data (basically the first and second derivative) is somewhat difficult at high temperatures. We therefore decided to use only the data from Burnham *et al.* and Schmidt. To reduce the random noise in α, the heat capacity data at low density were calculated from a sixth-order polynomial least square fit of S^r. At high density the heat capacity data were calculated directly from S^r, separately for each data source. However, the input data for the predictions at T_0, i.e., C_V^r, α, and $\partial C_V^r/\partial T$ were also calculated from a sixth-order polynomial fit of the merged entropy data set.

For methane we used the tables of Angus *et al.*[15] These tables were calculated on the basis of a 32-parameter equation of state, which was used also successfully for air, para hydrogen, nitrogen, oxygen (see Reynolds[16]) and Lennard-Jones fluids (see Nicolas *et al.*[17]). Values of C_V^r could be extracted directly from the tables, values of $\partial C_V^r/\partial T$ were calculated numerically around T_0. The covered part of the ρ,T diagram is represented in Fig. 3. Note that compared to water a relatively much larger temperature range is covered, taking into account the difference in critical temperature be-

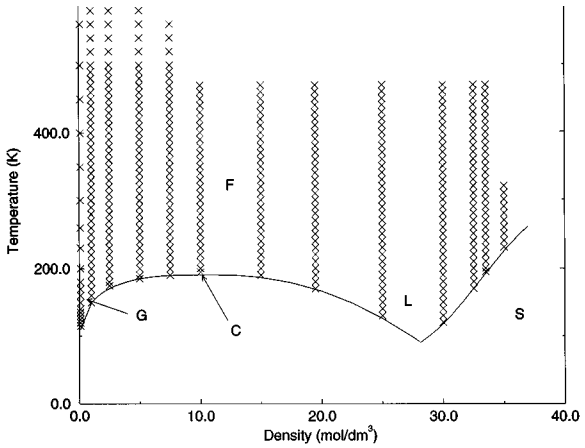

FIG. 3. The sampled part of the ρ,T diagram of methane. C denotes the critical point, and G, L, F, and S denote gas, liquid, fluid, and solid phase, respectively.

tween water (T_c=647.3 K) and methane (T_c=190.6 K).

Only for low density methane the exact Gamma state formulas [Eqs. (20)–(24), using the actual value of $\partial C_V^r/\partial T$ at T_0)] gave identical results to the effective Gamma state equations [Eqs. (20)–(24) with the effective δ_0^* calculated from Eq. (18)]. All other gas and typical liquid densities can thus be considered, if applicable, as *perturbed* Gamma states. We therefore use the effective Gamma state equations for all densities and the constant α and the confined Gamma approximations only for the more dense liquidlike systems. We will focus on low density water and methane first, then we will investigate high density systems, and finally we describe the behavior close to the critical point.

A. Low density water

In Fig. 4 the experimental values of S^r and C_V^r are given for water, together with the effective Gamma predictions.

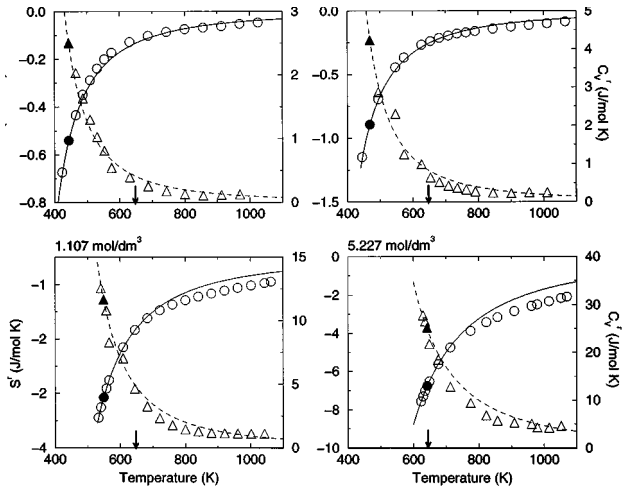

FIG. 4. Experimental results and effective Gamma predictions of S^r and C_V^r for low-density water. Legend: S^r experimental (○) and prediction (—); C_V^r experimental (△) and prediction (---). The values at the reference temperature T_0 are filled symbols; the critical temperature is denoted by an arrow.

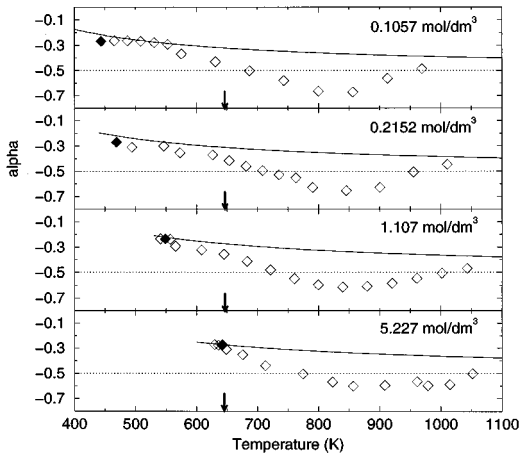

FIG. 5. Experimental results and effective Gamma predictions of α for low-density water. Legend: α experimental (◇) and prediction (—). The values at the reference temperature T_0 are solid symbols; the critical temperature is denoted by an arrow.

For low-density water up to ~0.4 mol/dm^3 the effective Gamma state is an excellent description for both S^r and C_V^r even for temperatures up to 1000 K. At densities above 1.0 mol/dm^3 (=0.018 kg/dm^3) there is a small but distinct deviation starting at ~800 K. All these low-density gases are described by negative Gamma states ($\delta_0^* < 0$ at T_0). As already mentioned the negative Gamma state can be considered only as an approximation of a more complex statistical state, valid up to a certain temperature. While initially, close to the coexistence line, the energy distribution is left-skewed, at a certain temperature it will become symmetric and for even higher temperatures it will transform itself into a right-skewed distribution. This is especially clear from the behavior of α in T, see Fig. 5. We see that close to the coexistence line, low-density water is described almost exactly by a negative Gamma state. For densities up to ~0.4 mol/dm^3 this holds for a temperature range of about 200 K. Above a certain temperature, the behavior of α starts to deviate from that of an effective negative Gamma state. We see that for all densities shown the real α crosses the line $-\frac{1}{2}$ at ~700 K, followed by a very shallow minimum of about -0.6 to -0.7 (corresponding to δ~0.3–0.4), indicating that $\rho(y)$ has transformed itself into a slightly right-skewed distribution. Above 1000 K, the thermodynamics is basically indistinguishable from that of the Gaussian state. By increasing the density to 5 mol/dm^3 we see that only the temperature range of ''perfect'' negative Gamma behavior is reduced, giving rise to a final 0.7 J mol^{-1} K^{-1} deviation in S^r at 1100 K for the last density. Also note that for the lowest densities the values of α close to the coexistence line are quite small (~−0.25), indicating that the initial distribution is rather asymmetric.

B. Low density methane

A similar behavior is observed for low-density methane, but in details different because of the different type of mo-

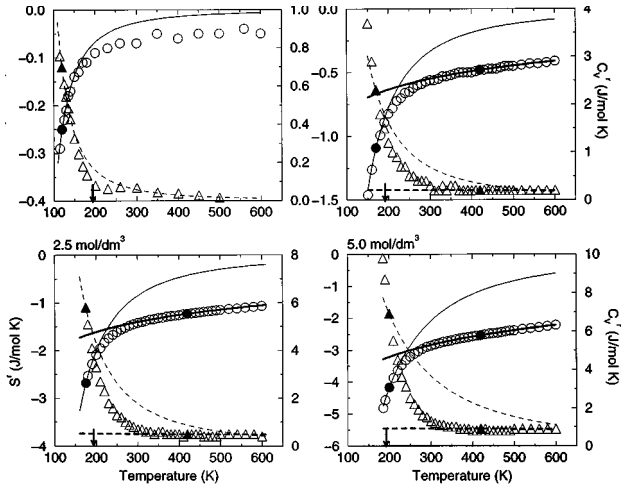

FIG. 6. Experimental results and effective Gamma predictions of S^r and C_V^r for low-density methane. Legend: S^r experimental (○) and predictions with low T_0 (—) and high T_0 (—); C_V^r experimental (△) and predictions with low T_0 (---) and high T_0 (---). The values at both reference temperatures T_0 are denoted by solid symbols; the critical temperature is denoted by an arrow.

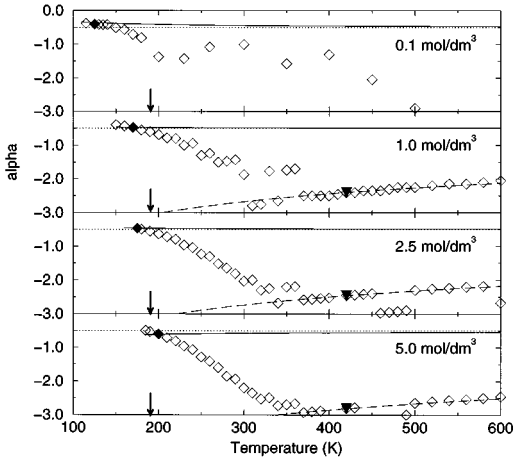

FIG. 7. Experimental results and effective Gamma predictions of α for low-density methane. Legend: α experimental (◇) and predictions with low T_0 (—) and high T_0 (---). The critical temperature is denoted by an arrow; the T_0's by solid symbols.

lecular interactions. In Fig. 6 the experimental values and the effective Gamma predictions of S^r and C_V^r are presented, using a T_0 close to the coexistence line. First of all we see that in the first 60 K, say, starting from the coexistence line, the effective Gamma is in good agreement with the experimental entropy data for all densities presented, although the deviations for the heat capacity are larger. Furthermore, it is clear that, in contrast with water, already at the lowest density there is a distinct deviation at higher temperature. Just like water, the deviations are more pronounced at higher densities. Interestingly, if we look at the temperature range ΔT within which the entropy is more or less well described, we find that for ρ=1.0–5.0 mol/dm^3 (=0.016–0.080 kg/dm^3) the normalized quantity $\Delta T/T_c$ for methane (0.26–0.32) is virtually the same as for water (0.31–0.35). The behavior of α is given in Fig. 7. We see that close to the coexistence line the system is also described by a negative Gamma state, although less asymmetric than water ($\alpha\sim-0.4$). We see also in this case that there is a transition from a moderately left-skewed distribution via a symmetric towards a quite asymmetric right-skewed one ($\alpha\sim-3$, corresponding to $\delta\sim0.98$). If we choose a higher reference temperature (T_0=420 K) we obtain for all gas densities presented a positive Gamma state, which is perfectly able to describe the high temperature data (S^r,C_V^r as well as α) over a large range (250–600 K), see Figs. 6 and 7. Of course below a certain temperature the agreement breaks down. From Figures 6 and 7 it is clear that after the transformation from a left to a right-skewed distribution, a stable positive Gamma state is obtained. The same is true also for low-density water, although there the stable positive Gamma state is almost a Gaussian state ($\alpha\sim-0.5$).

C. High density water

Next we will focus on high-density systems. For liquid water the results of the effective Gamma, constant alpha and the confined Gamma equations are compared to experimental data in Figs. 8 and 9 for densities ranging from 0.55 g/cm^3 to 0.997 g/cm^3.

For all four densities the confined Gamma predictions agree very well with both the experimental entropy and heat capacity data, even for a temperature range of 500 K. Both the effective Gamma and the constant alpha approximations reproduce the entropy data over 200–300 K very well, but deviate somewhat for larger temperature ranges. It is clear that the quality of the constant alpha approximation improves with increasing density. The experimental heat capacity data from Schmidt and Burnham *et al.* are given separately, to indicate the noise and discrepancies in the experimental C_V' data, especially at lower density, when calculated directly from the entropy. For the heat capacity the effective Gamma approximation is less accurate than the confined Gamma one, while for higher densities the constant alpha approximation is comparable. This confirms our previ-

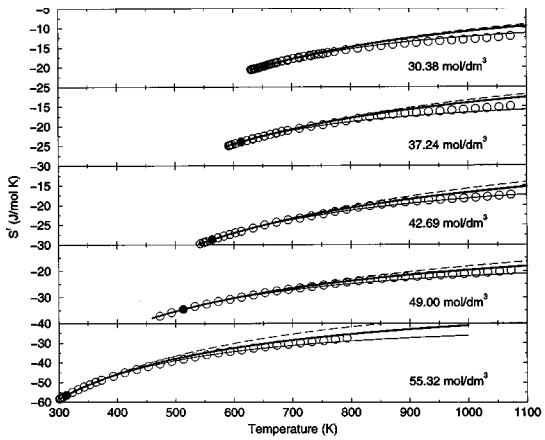

FIG. 8. Experimental results and predictions of S^r for high-density water. Legend: S^r experimental (○) and effective Gamma (---), confined Gamma (—), and constant alpha predictions (—). The value at the reference temperature T_0 is denoted by solid symbols.

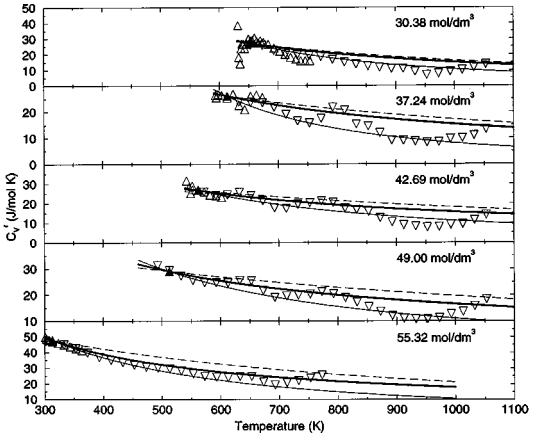

FIG. 9. Experimental results and predictions of C_V^r for high-density water. Legend: C_V^r experimental from Schmidt (Ref. 11) (△) and Burnham *et al.* (Ref. 12) (▽) and effective Gamma (---), confined Gamma (—), and constant alpha predictions (—). The value at the reference temperature T_0 is denoted by solid symbols.

ous findings on liquid water[1] at 55 mol/dm^3. Maybe the ''waves'' in the experimental C_V^r data from Burnham *et al.* are caused by the particular choice of the analytical shape of the equation of state they used to produce their tables. For all densities the confined Gamma approximation seems to be the best curve through the experimental data. In Fig. 10 the experimental values of α are presented with the various predictions. The values of α were calculated separately for each source. Even for α the confined Gamma prediction is about the best curve through the (noisy) experimental points for every density. We see that with increasing density α becomes more constant in temperature. This explains why the quality of the constant alpha approximation is enhanced with density. For 55 mol/dm^3 we see that this constant alpha approximation is almost exact.

In Table I we present the parameters of the effective Gamma and confined Gamma state. Note that in the tables

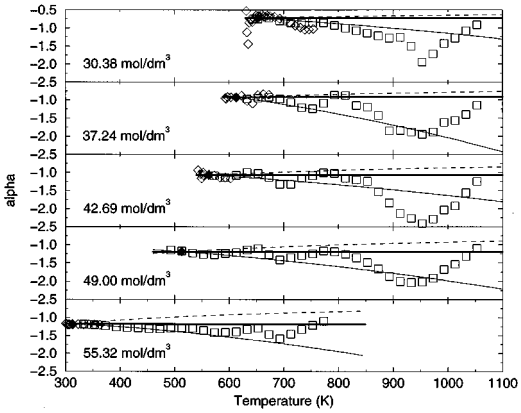

FIG. 10. Experimental results and predictions of α for high-density water. Legend: α experimental from Schmidt (Ref. 11) (◇) and Burnham *et al.* (Ref. 12) (□) and effective Gamma (---), confined Gamma (—), and constant alpha predictions (—). The value at the reference temperature T_0 is denoted by solid symbols.

TABLE I. Gamma state parameters of high-density water at T_0.

ρ (mol/dm^3)	T_0 (K)	δ_0[a]	$\overline{\epsilon}$[a]	δ_0^*[a]
30.38	653.0	−0.13(−0.23)	0.42 (0.37)	0.44 (0.48)
37.24	613.0	−0.26(0.22)	0.21 (0.35)	0.63 (0.66)
42.69	563.0	0.30(0.44)	0.24 (0.33)	0.72 (0.72)
49.00	513.0	0.34(0.49)	0.15 (0.24)	0.77 (0.76)
55.32	313.0	0.49(0.57)	0.09 (0.14)	0.77 (0.77)

[a]Calculated from a sixth-order polynomial fit on S^r; values between parentheses are calculated from a second-order fit on crude experimental C_V^r data.

we give the molecular phase-space fraction $\overline{\epsilon}=\epsilon^{1/N}$, with N the total number of molecules in the system. As an illustration of the errors in these parameters the values of C_V^r and $\partial C_V^r/\partial T$ were also calculated via a second-order polynomial fit on the merged C_V^r data from Schmidt and Burnham *et al.*, instead of via a sixth-order polynomial fit on the merged S^r data. This gave a second set of parameters δ_0, $\overline{\epsilon}$, and δ_0^* at T_0, see the values in Table I between parentheses. Comparing the two sets we see that they are quite close. It is also clear that the confined Gamma state at the two lowest liquid densities is not completely defined: the value of δ_0 is very close to zero, being either negative or positive depending on the precise input data. In fact, these exact Gamma states are almost Gaussian ones.

To illustrate the effect of the density on the energy distribution we calculated the values of δ, δ^*, and α at a common temperature, namely 653 K, see Table II. In addition, the values of $\overline{\epsilon}$ were calculated again and matched very well the values evaluated at T_0 (Table I), as the volume fraction of occupied phase space should be temperature independent. Here we must stress that for this temperature the value of $\partial C_V^r/\partial T$ at 55 mol/dm^3 was more difficult to evaluate with the same precision than at lower densities, because of the large noise in the experimental data. Remember that for this density the temperature is ~350 K away from the coexistence line, and the experimental data are measured at pressures exceeding 8000 bar. A worse evaluation of $\partial C_V^r/\partial T$ will especially influence the calculation of $\epsilon=\exp[(S^r-S^{\Gamma r})/k]$. Anyway, the values of δ of the confined Gamma state clearly increase with density, the system at 30 mol/dm^3 still being represented by a negative Gamma state, but for all other densities by a positive one. The increase of δ with density is a reflection of the fact that the potential energy distribution in water becomes more asymmetric by increasing the density, since the average intermolecular distances are somewhat reduced, which gives rise to more unfavourable interactions. In this way the right (high energy) tail of $\rho(y)$ becomes more pronounced, while the distribution close to the mode is only little affected since water, because of its very directed and strong interactions, is able to maintain on average a reasonable low-energy structure on increasing density. At the same time we see the value of $\overline{\epsilon}$ decreasing from ~40% to ~10% of phase space, as expected from the fact that the number of configurations with a not too unfavourable potential energy will decrease with density. For the

TABLE II. Gamma state parameters of high-density water at 653 K.

ρ (mol/dm^3)	ρ/ρ_c[a]	$\delta(653)$[b]	$\overline{\epsilon}(653)$[b]	$\delta^*(653)$[b]	$\alpha(653)$[b]
30.38	1.74	−0.23	0.37	0.48	−0.75
37.24	2.13	0.15	0.32	0.66	−0.96
42.69	2.44	0.28	0.26	0.74	−1.11
49.00	2.80	0.36	0.20	0.80	−1.26
55.32	3.16	~0.57	~0.22	0.84	−1.40

[a]Reduced density, using a critical density ρ_c of 17.51 mol/dm^3 (Ref. 11).
[b]Values of the double state and effective δ, the molecular phase-space fraction $\overline{\epsilon}$, and α calculated at $T=653.0$ K from a second-order fit on crude experimental C_V^r data.

same reason the value of the effective δ^* at 653 K (Table II) increases with density, partly to correct for the increasing extra term $k \ln \epsilon$ in the entropy due to the growing unstable part of phase space. Basically, in the effective Gamma state the value of $M_3 \propto \partial C_V^r/\partial T$ is adapted to reproduce the entropy at T_0, keeping fixed the value of $M_2 \propto C_V^r$. Furthermore, the values of $|\alpha|$ increase with density, indicating a larger ''resistance'' of high density systems for increasing the order when the temperature is lowered [see also Eq. (13)]. This means that at comparable temperature systems at higher density already have a more collapsed structure which, decreasing the temperature, cannot be easily optimized.

D. High density methane

For high density methane the results of the predictions of S^r and C_V^r are presented in Figs. 11 and 12, using the effective Gamma, the confined Gamma and the constant alpha approximations. As T_0 we choose a temperature above which the behavior of C_V^r was ''regular'' i.e., decreasing with temperature (see Fig. 12).

In Fig. 11 we see that all three approximations agree very well with the experimental S^r data, even for temperatures ~200 K lower than T_0. The only exception is the constant alpha approximation at 30 mol/dm^3, which is only valid up to ~100 K below T_0. For the heat capacity, especially the confined Gamma approximation reproduces the experimental data very well above T_0, and just as in the case of water for higher densities, the constant alpha approximation is also very accurate. Similar to water we see that the effective Gamma state, although very good for the entropy, shows more deviations for the heat capacity. In Fig. 13 the experimental values of α and the different predictions are given. We see that in all cases the confined Gamma approximation gives very good results over a large temperature range; at higher density also the constant alpha approximation works well. Remember that α, being the ratio of two quantities, is the most sensitive property. We see that just as with water the stability of α is enhanced with density.

In Table III the parameters of the confined and effective Gamma states at T_0 are given and in Table IV the values of these parameters are presented at a common temperature (320 K). First of all it is clear that, although in absolute terms the densities of ''regular'' liquid water and methane are comparable (starting at ~30 mol/dm^3), the reduced densities ρ/ρ_c are much larger for methane than for water (see Tables II and IV). Here the critical densities are $\rho_c=10.11$ mol/dm^3 for methane[15] and 17.51 mol/dm^3 for water.[13] This is (probably) caused by the much weaker interactions in methane.

Secondly we see that the values of both δ and δ^* (Table IV) are much larger than for water (Table II), indicating that the potential energy distribution in methane is much more

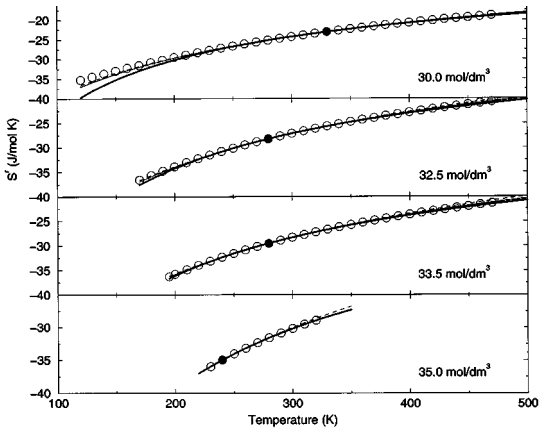

FIG. 11. Experimental results and predictions of S^r for high-density methane. Legend: S^r experimental (○) and effective Gamma (---), confined Gamma (—) and constant alpha predictions (—). The value at the reference temperature T_0 is denoted by solid symbols.

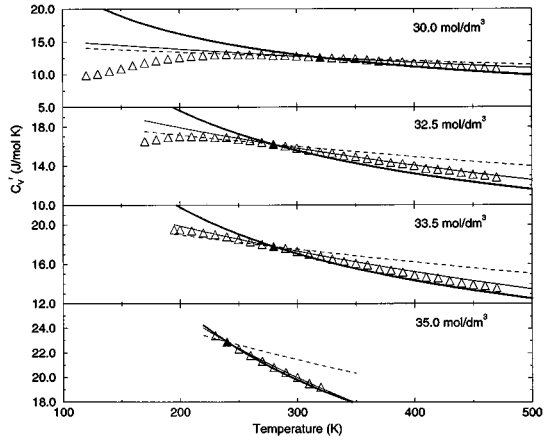

FIG. 12. Experimental results and predictions of C_V^r for high-density methane. Legend: C_V^r experimental (△) and effective Gamma (---), confined Gamma (—) and constant alpha predictions (—). The value at the reference temperature T_0 is denoted by solid symbols.

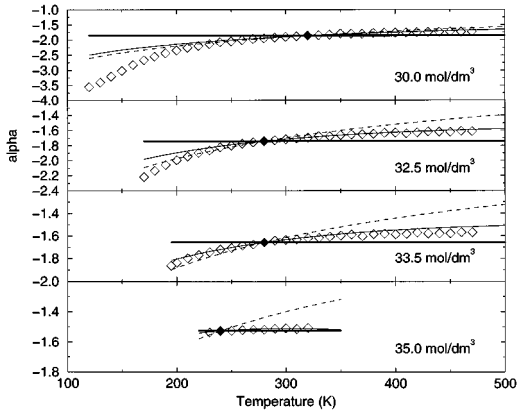

FIG. 13. Experimental results and predictions of α for high-density methane. Legend: α experimental ($\diamond$) and effective Gamma (---), confined Gamma (—), and constant alpha predictions (—). The value at the reference temperature T_0 is denoted by solid symbols.

asymmetric i.e., quite ''thin'' around the mode and with a long tail on the right (high energy) side. This stronger asymmetry can be explained by the fact that the intermolecular interactions in methane are of much shorter range and the attractive interactions are much weaker (compared to the repulsive ones) than in water. Hence, at relatively high density the weight of the high energy values in methane is larger than in water, where the dominating long-range electrostatic interactions create more or less a balance between attraction and repulsion, giving rise to a more symmetric distribution.

Also we see that the values of the molecular volume fraction $\overline{\epsilon}$ of the stable region in Tables III and IV are in reasonable agreement, decreasing from ~60% to ~30% of phase space. These values are significantly larger than for water. The reason for this could be simply the difference in intermolecular interactions. Methane can be represented very well by a monoatomic van der Waals liquid with virtually no directional preferences,[7,18] whereas water forms hydrogen bonded structures with very directed interactions. Because of this very strong ordering in water the fraction of configurations with a ''favorable'' energy (inside the confined Gamma state) is much less than in the case of methane, where the intermolecular distance is the determining factor and the angular orientations are much less important.

Interestingly, we see that by increasing the density the values of δ and δ^* are actually decreasing. This indicates that in contrast with water the second moment of the energy distribution of methane is increasing faster than the third one (remember that $\delta = M_3/2kTM_2$, see Eqs. (9) and (17), i.e., the distribution is getting ''fatter'' around the mode, instead of enhancing the asymmetry. We also see that the absolute value of α is decreasing with density; hence C_V^r ($\propto M_2$) is increasing faster than the order in the system ($-S^r$); in water we see the opposite. Probably for a simple system like methane the order can be hardly increased (S^r be decreased) with density as the intermolecular distance is the dominant factor for the potential energy. Water, on the other hand, can still optimize the structure much more at high density, as the orientation of the molecules is also very important. From this it follows that for liquids consisting of molecules of intermediate polarity α might be quite constant in density.

TABLE III. Gamma state parameters of high-density methane at T_0.

ρ (mol/dm^3)	T_0 (K)	δ_0	$\overline{\epsilon}$	δ_0^*
30.0	320.0	0.87	0.64	0.92
32.5	280.0	0.83	0.47	0.90
33.5	280.0	0.81	0.47	0.89
35.0	240.0	0.72	0.28	0.87

E. Intermediate densities

For intermediate densities we find a more complex behavior of the thermodynamic properties. For water approximately up to the critical point the behavior of C_V^r is regular, i.e., decreasing with temperature. Around the critical density though we find that C_V^r starts to behave differently; close to the coexistence line it increases with temperature but after some temperature interval it behaves regular again (see for example the initial behavior of C_V^r at 30 mol/dm^3, Fig. 9). For methane the behavior of C_V^r above the critical density (10 mol/dm^3) to ~30 mol/dm^3 is given in Fig. 14. We see that only above 30 mol/dm^3 there is a regular behavior at high temperature within the range of experimental data. Clearly, the behavior around the critical point cannot be described by a simple Gamma state (being either effective Gamma or confined Gamma). This means that neither the entire phase space can be described by one single (effective) Gamma state, nor the system is confined within a small stable part of phase space (confined Gamma). Maybe in such conditions a full double state model, using two Gamma states, is able to describe properly the behavior of the system.

TABLE IV. Gamma state parameters of high-density methane at 320 K.

ρ (mol/dm^3)	ρ/ρ_c[a]	$\delta(320)$[b]	$\overline{\epsilon}(320)$[b]	$\delta^*(320)$[b]	$\alpha(320)$[b]
30.0	2.97	0.87	0.64	0.92	−1.86
32.5	3.21	0.84	0.61	0.89	−1.70
33.5	3.31	0.76	0.40	0.88	−1.62
35.0	3.46	0.71	0.34	0.86	−1.51

[a]Reduced density, using a critical density ρ_c of 10.11 mol/dm^3 (Ref. 13).
[b]Values of the double state and effective δ, the molecular phase-space fraction $\overline{\epsilon}$, and α calculated at $T=320$ K from the experimental S^r and C_V^r data.

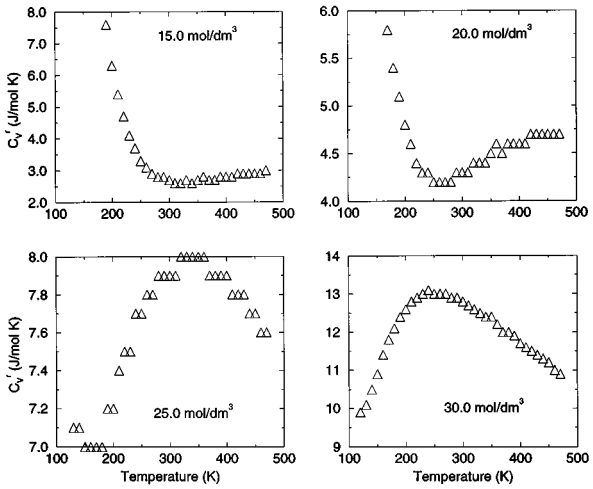

FIG. 14. Experimental results of C_V^r for methane beyond the critical density.

IV. DISCUSSION AND CONCLUSIONS

In this paper we presented an investigation of the applicability of the quasi-Gaussian entropy theory on two very different systems, water and methane. For densities ranging from the almost ideal gas to dense liquids we calculated experimental *reduced* thermodynamic properties (basically entropy S^r, heat capacity C_V^r, and the intrinsic entropy function $\alpha = S^r/C_V^r$) and compared them with various predictions following from the theory. If the statistical state of the system is a weakly perturbed Gamma state, the effective Gamma and the confined Gamma approximations can be used. A third approach is the constant alpha approximation. We showed in this paper that a large part of the ρ, T diagram of water and methane can be considered as weakly perturbed Gamma states, where the effective Gamma or confined Gamma equations give good results. This is schematically illustrated in Fig. 15, giving the effective Gamma regions.

For low density systems we find close to the coexistence line a weakly perturbed *negative* Gamma state (due to the fact that at this low density the repulsive interactions are hardly present and only attractive interactions, i.e., negative potential energies, occur). At higher temperatures the repulsive interactions are becoming more important, and within a small temperature interval the system transforms itself into a weakly perturbed *positive* Gamma state, which can be described accurately by an effective Γ_+ state. Probably this effective Gamma state is able to describe the physics of the system at every temperature above the $\Gamma_- \rightarrow \Gamma_+$ transition. Therefore for typical gas densities the entire phase-space can be described by one effective Γ state ($\epsilon \approx 1$). For very dilute systems the statistical state of the system is an exact negative Gamma state at every temperature and in the limit of infinite dilution the left-skewed Gamma distribution will become a delta function [i.e., a (negative) Gamma distribution with $M_3 \propto b_1 \propto \delta \rightarrow 0$ and also $C_V^r \propto M_2 \rightarrow 0$]. For larger densities the temperature range of applicability of the effective Γ_- state decreases, while the range of the high-temperature effective Γ_+ state increases.

For densities close to the critical density, the effective Γ_+ state is not able to describe the behavior of the system any more. This can be explained in terms of the double state model: phase space can be split into two regions of still comparable free energy, where one of the regions is described by an exact Gamma state, but the second one has an unknown statistical state. Perhaps it is possible to describe also this second region by another Gamma state, but this is something which has to be investigated more thoroughly.

For densities beyond the critical density this second region of phase space becomes very unstable with respect to the Gamma state, i.e., the system is completely confined within one part of phase space, the confined Gamma region. Probably this confinement reflects the appearing molecular restrictions of the system. We see that the volume fraction of this stable part of phase space (ϵ) decreases with density, as with increasing density the fraction of the very unstable configurations is enlarged very much. For methane the confined Gamma states are Γ_+ ones, with a large δ ($\sim$0.7 to 0.9), while for water the exact Gamma state is either slightly negative (lowest density) or moderately positive ($\delta \sim -0.2$ to 0.5). This difference in asymmetry of the potential energy distribution is caused by the difference in intermolecular potential (short range, only weakly attractive van der Waals interactions in methane and long-range electrostatic interactions in water, where the attractive interactions are of the same magnitude as the repulsive ones).

This partitioning explains the fact that the entire phase space in the fluid-liquid regime can be described by a perturbed Gamma state. The effective Γ_+ state therefore is able to reproduce the entropy very well (and, hence, the free energy[1]) but less accurately the heat capacity. An interesting feature of these fluid-liquid systems is the fact that the intrinsic entropy function α is becoming very stable in temperature for high density systems. Therefore, in this range of densities also the constant alpha approximation gives very good results.

For solids with, in general, an even higher density, we find in the classical limit (''ideal'' classical harmonic solid) again an exact Γ_+ state.[1] This exact ''harmonic'' Γ_+^h state has a nonconverging free energy, as the atoms may be infi-

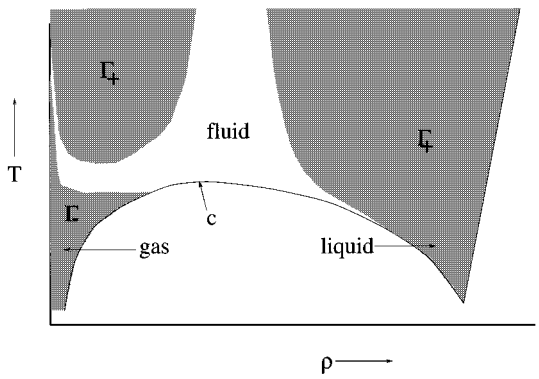

FIG. 15. A schematic phase-diagram of water (methane) with an indication of the regions where one of the two effective Gamma states (Γ_+ or Γ_-) is applicable. c denotes the critical point.

nitely far apart. In a real monatomic solid, behaving almost like a classical harmonic solid (i.e., $C_V \approx 3R$, $C_V^r \approx \frac{3}{2}R$ and $\partial C_V^r/\partial T \approx 0$), this is obviously not the case. Indeed in a real solid the system is confined into a small part of phase space, just as in the case of liquids. The statistical state of this small part of phase space is a converging state, well approximated by the Γ_+^h state. The value of ϵ is likely to be even smaller than for dense liquids.

Interestingly the idea of ''confinement'' of a liquid system into a small part of phase space is also expressed in several other models of the liquid state. One of the simplest cell models is the Lennard-Jones and Devonshire model,[18] where each molecule is confined to its own ''cell'' and the configuration partition function $\mathcal{Q}$ is split into partition functions of single occupancy and a disorder parameter. The molecules are thought to move in the field produced by the neighbouring ones as if they were fixed at the centers of their cells. Another model is the one proposed by Eyring *et al.*,[19–21] where the degrees of freedom of the system are arbitrarily divided into ''crystallike'' and ''gaslike'' ones.

In general, we can say that in this paper we have shown that in a large part of the ρ, T phase diagram there is a general description of thermodynamic properties in terms of simple Gamma states (effective Gamma or confined Gamma). It is also clear that the temperature range of applicability is very large: in many cases excellent predictions of various properties over a range of more than 500 K are possible. This means that for different densities properties can be measured at relatively moderate conditions, not very far from the coexistence line, and extrapolated to for example supercritical conditions. This could therefore be used to construct an equation of state valid over a large temperature range. Existing equations of state can be examined for consistency with our description. It is also clear that the description is valid for molecules with very different chemical properties, like water (very polar) and methane (very apolar). Furthermore, the theory can be applied to the overall properties of mixtures as well, and can also be formulated for partial molar properties. Presently we are investigating the partial molar properties of a solute at infinite dilution.

ACKNOWLEDGMENTS

We like to thank Dr. J. Mavri (National Institute of Chemistry, Slovenia) and Professor A. Di Nola (Rome) for a careful reading of the manuscript and stimulating discussions. This work was supported by the Netherlands Foundation for Chemical Research (SON) with financial aid from the Netherlands Organization for Scientific Research (NWO) and by the Training and Mobility of Researchers (TMR) Program of the European Community.

APPENDIX A: HIGH TEMPERATURE LIMIT OF α

The intrinsic entropy function α can be expressed in properties of the elementary subsystem as[1]

$$\alpha(\beta) = -\frac{\ln[1+\mu_2(\beta^2/2!)+\mu_3(\beta^3/3!)+\cdots]}{\mu_2\beta^2}, \qquad \text{(A1)}$$

where μ_n is the nth central moment of the potential energy fluctuation $\Delta\epsilon$ within each elementary subsystem. Since we are interested in the limit $T\to\infty$, i.e., $\beta\to 0$ we must know the behavior of μ_n in T. In general, we can decompose the energy distribution function as $\rho(\Delta\epsilon)=\exp(-\beta\epsilon)\Omega\epsilon/q$, where $\Omega(\epsilon)$ is the microcanonical partition function at energy ϵ, q is the usual canonical partition function of the elementary system and $\exp(-\beta\epsilon)$ is the Boltzmann factor.[10] Since $\Omega(\epsilon)$ is temperature independent and the Boltzmann factor tends to one as $\beta\to 0$ we find

$$\lim_{\beta\to 0}\mu_n = \lim_{\beta\to 0}\frac{\int(\Delta\epsilon)^n\Omega(\epsilon)\exp(-\beta\epsilon)d\epsilon}{\int\Omega(\epsilon)\exp(-\beta\epsilon)d\epsilon} = \frac{\int(\Delta\epsilon)^n\Omega(\epsilon)d\epsilon}{\int\Omega(\epsilon)d\Delta\epsilon}. \qquad \text{(A2)}$$

This means that the moments (if existing) reach a final value at infinite temperature. The assumption that these moments exist is generally accepted in perturbation theory see, for example, Zwanzig[22] or Hansen and McDonald.[7] Therefore, since all moments reach a final finite value, the argument of the logarithm in Eq. (A1) tends to one, and by expanding we find

$$\lim_{\beta\to 0}\alpha(\beta) = -\tfrac{1}{2}. \qquad \text{(A3)}$$

It still depends on the sign of μ_3 from which side this limiting value is reached. If $\mu_3<0$, i.e., a left-skewed distribution, the limit is approached from the right, and vise versa for right-skewed distributions.

APPENDIX B: DOUBLE STATE MODEL

In this appendix we introduce the basic idea of a partitioning of phase space into two different regions.

The ideal reduced free energy can be written as[1]

$$A' = -kT\ln\mathcal{Q}' = -kT\ln\frac{\mathcal{Q}}{\mathcal{Q}_0}, \qquad \text{(B1)}$$

where $\mathcal{Q}$ and $\mathcal{Q}_0$ are the partition functions of the system and the reference state and $\mathcal{Q}'$ is the reduced partition function. If we (arbitrarily) subdivide the phase space into two regions, called ''a'' and ''b'', we get

$$\mathcal{Q} = \mathcal{Q}^a + \mathcal{Q}^b \qquad \text{(B2)}$$

and a similar expression for $\mathcal{Q}_0$. Hence, we can rewrite Eq. (B1) as

$$A' = -kT\ln\left(\frac{\mathcal{Q}^a}{\mathcal{Q}_0^a}\frac{\mathcal{Q}_0^a}{\mathcal{Q}_0} + \frac{\mathcal{Q}^b}{\mathcal{Q}_0^b}\frac{\mathcal{Q}_0^b}{\mathcal{Q}_0}\right) = -kT\ln[\epsilon e^{-\beta A^{a'}} + (1-\epsilon)e^{-\beta A^{b'}}], \qquad \text{(B3)}$$

where $\epsilon = \mathcal{Q}_0^a/\mathcal{Q}_0$ is the volume-fraction of phase space belonging to the a region. This volume-fraction is temperature independent, since the reference state (with no interactions and no vibrations) can be regarded as a system at infinite temperature, as the effect of $\mathcal{V}\to 0$ is the same as $\beta\to 0$. Therefore $\mathcal{Q}_0$ is just the phase-space volume. Further

$A^{a'} = -kT \ln \mathcal{Q}^a/\mathcal{Q}_0^a$ is the ideal reduced free energy of the a region, $A^{b'}$ is the ideal reduced free energy of the b region.

We can obtain the other thermodynamic properties using $S' = (\partial A'/\partial T)_V$, $U' = A' + TS'$, and $C_V' = (\partial U'/\partial T)_V$. This yields

$$S' = k \ln[\epsilon e^{-\beta A^{a'}} + (1-\epsilon) e^{-\beta A^{b'}}] + \frac{\epsilon e^{-\beta A^{a'}} U^{a'} + (1-\epsilon) e^{-\beta A^{b'}} U^{b'}}{T\mathcal{Q}'}, \tag{B4}$$

$$U' = \frac{\epsilon e^{-\beta A^{a'}} U^{a'} + (1-\epsilon) e^{-\beta A^{b'}} U^{b'}}{\mathcal{Q}'}, \tag{B5}$$

$$C_V' = \frac{\epsilon e^{-\beta A^{a'}} C_V^{a'} + (1-\epsilon) e^{-\beta A^{b'}} C_V^{b'}}{\mathcal{Q}'} + \frac{\epsilon e^{-\beta A^{a'}} (U^{a'}) + (1-\epsilon) e^{-\beta A^{b'}} (U^{b'})^2}{kT^2 \mathcal{Q}'} - \frac{1}{kT^2}\left\{\frac{\epsilon e^{-\beta A^{a'}} U^{a'} + (1-\epsilon) e^{-\beta A^{b'}} U^{b'}}{\mathcal{Q}'}\right\}^2 \tag{B6}$$

with

$$\mathcal{Q}' = \epsilon e^{-\beta A^{a'}} + (1-\epsilon) e^{-\beta A^{b'}}. \tag{B7}$$

The energy distribution function of the entire phase space is given by

$$\rho(\mathscr{V}) = \frac{\epsilon e^{-\beta A^{a'}} \rho^a(\mathscr{V}) + (1-\epsilon) e^{-\beta A^{b'}} \rho^b(\mathscr{V})}{\mathcal{Q}'} \tag{B8}$$

as can be checked easily by calculating $\langle \exp(\beta \mathscr{V}) \rangle$ and realizing that $\langle \exp(\beta \mathscr{V}) \rangle_a - \equiv \exp(\beta A^{a'})$ and $\langle \exp(\beta \mathscr{V}) \rangle_b \equiv \exp(\beta A^{b'})$, where $\langle \cdots \rangle_a$ and $\langle \cdots \rangle_b$ are ensemble averages in the a and b region.

If the free energy of the b region is much higher than the free energy of the a region, then $(1-\epsilon)\exp(-\beta A^{b'})$ is negligible with respect to $\epsilon \exp(-\beta A^{a'})$, which means that the system is completely confined into the a region. If, furthermore, we assume that the statistical state of the a region is a Gamma state, Eqs. (B3)–(B6) can be simplified to the *confined Gamma* equations:

$$A' = A^{\Gamma'} - kT \ln \epsilon, \tag{B9}$$

$$S' = S^{\Gamma'} + k \ln \epsilon, \tag{B10}$$

$$U' = U^{\Gamma'}, \tag{B11}$$

$$C_V' = C_V^{\Gamma'}, \tag{B12}$$

where $C_V^{\Gamma'}$, $S^{\Gamma'}$, $U^{\Gamma'}$, and $A^{\Gamma'}$ are given by Eqs. (21)–(24). We see that in this case the entropy is just the entropy of an exact Gamma state with a constant temperature independent shift. Moreover, for the free energy there is a correction term. With the knowledge of U_0', C_{V0}', $\partial C_{V0}'/\partial T$, and S_0' at the reference temperature T_0 one can calculate the phase-space volume fraction ϵ, using Eq. (B10).

Within the same approximation we find that Eq. (B8) simplifies to

$$\rho(\mathscr{V}) = \rho^{\Gamma}(\mathscr{V}), \tag{B13}$$

where $\rho^{\Gamma}(\mathscr{V})$ is the Gamma distribution of the Γ region, implying that this approach corresponds to perturbed Gamma state conditions, in the whole phase space.

In molecular terms the confined Gamma region probably for a large part corresponds to ''ordered'' molecular clusters or structures, while the other part of phase space corresponds to high-energy configurations.

[1] A. Amadei, M. E. F. Apol, A. Di Nola, and H. J. C. Berendsen, J. Chem. Phys. **104**, 1560 (1996).
[2] J. K. Ord, *Families of Frequency Distributions* (Griffin, London, 1972).
[3] With ''no vibrations'' we actually mean zero vibrational energies, although the quantum phase space is still present.
[4] N. I. Johnson and S. Kotz, *Discrete distributions* (Houghton Mifflin, New York, 1969).
[5] M. Abramowitz, and I. Stegun, *Handbook of Mathematical Functions* (Dover, New York, 1972).
[6] R. C. Tolman, *The Principles of Statistical Mechanics* (Oxford University Press, London, 1938).
[7] J. P. Hansen, and I. R. McDonald, *Theory of simple Liquids*, 2nd Ed. (Academic, London, 1986).
[8] The proof is simple, since $\partial C_V'/\partial T = -2C_{V0}' T_0^2 (1-\delta_0)/[T(1-\delta_0) + T_0\delta_0]^3$, which is always negative as the denominator is always positive for a Γ_+ and positive for all $T > T_*$ for a Γ_- distribution.
[9] E. F. Obert and R. A. Gaggioli, *Thermodynamics*, 2nd Ed. (McGraw-Hill, New York, 1963).
[10] J. E. Mayer, and M. G. Mayer, *Statistical Mechanics* (Wiley, New York, 1940).
[11] L. H. Jones and R. S. McDowell, J. Mol. Spectrosc. **3**, 632 (1959).
[12] R. S. McDowell and F. H. Kruse, J. Chem. Eng. Data **8**, 547 (1963).
[13] E. Schmidt, *Properties of Water and Steam in SI-units* (Springer-Verlag, Berlin, 1969).
[14] C. W. Burnham, J. R. Holloway, and N. F. Davis, *Thermodynamic Properties of Water to 1000 °C and 10 000 Bars*, (Geological Society America, Boulder, CO., 1969), Special paper No. 132.
[15] S. Angus, B. Armstrong, and K. M. de Reuck, *Methane*, Vol. 5 of *International Thermodynamic Tables of the Fluid State* (Pergamon, Oxford, 1976).
[16] W. C. Reynolds, *Thermodynamic Properties in SI* (Department of Mechanical Engineering, Stanford University, Stanford, CT, 1979).
[17] J. J. Nicolas, K. E. Gubbins, W. B. Streett, and D. J. Tildesley, Mol. Phys. **37**, 1429 (1979).
[18] F. Kohler, *The Liquid State* (Verlag Chemie, Weinheim, 1972).
[19] H. Eyring, T. Ree, and N. Hirai, Proc. Nat. Acad. Sci. **44**, 683 (1958).
[20] T. S. Ree, T. Ree, and H. Eyring, Proc. Nat. Acad. Sci. **48**, 501 (1962).
[21] *Liquids: Structure, Properties, Solid Interactions*, edited by T. J. Hughel (Elsevier, Amsterdam, 1965); Proceedings of the Symposium held at General Motors Research Laboratories, Warren, Michigan, 1963.
[22] R. W. Zwanzig, J. Chem. Phys. **22**(8), 1420 (1954).